Pergamon

Bioorganic & Medicinal Chemistry, Vol. 4, No. 9, pp 1471–1480, 1996

PII: S0968-0896(96)00140-X
0968-0896/96 $15.00+0.00

Structure-Based Design of Achiral, Nonpeptidic Hydroxybenzamide as a Novel P2/P2′ Replacement for the Symmetry-Based HIV Protease Inhibitors

Ramnarayan S. Randad,* Lucyna Lubkowska, Abelardo M. Silva, Diego M. A. Guerin,† Sergei V. Gulnik, Betty Yu and John W. Erickson

Structural Biochemistry Program, SAIC-Frederick, National Cancer Institute—Frederick Cancer Research and Development Center, Frederick, MD 21702, U.S.A.

Abstract—A combination of structure–activity studies, kinetic analysis, X-ray crystallographic analysis, and modeling were employed in the design of a novel series of HIV-1 protease (HIV PR) inhibitors. The crystal structure of a complex of HIV PR with *SRSS*-2,5-bis[*N*-(*tert*-butyloxycarbonyl)amino]-3,4-dihydroxy-1,6-diphenylhexane (**1**) delineated a crucial water-mediated hydrogen bond between the *tert*-butyloxy group of the inhibitor and the amide hydrogen of Asp29 of the enzyme. Achiral, nonpeptidic 2-hydroxyphenylacetamide and 3-hydroxybenzamide groups were modeled as novel P2/P2′ ligands to replace the crystallographic water molecules and to provide direct interactions with the NH groups of the Asp29/129 residues. Indeed, the symmetry-based inhibitors **7** and **19**, possessing 3-hydroxy and 3-aminobenzamide, respectively, as a P2/P2′ ligand, were potent inhibitors of HIV PR. The benzamides were superior in potency to the phenylacetamides and have four fewer rotatable bonds. An X-ray crystal structure of the HIV PR/**7** complex at 2.1 Å resolution revealed an asymmetric mode of binding, in which the 3-hydroxy group of the benzamide ring makes the predicted interaction with the backbone NH of Asp29 on one side of the active site only. An unexpected hydrogen bond with the Gly148 carbonyl group, resulting from rotation of the aromatic ring out of the amide plane, was observed on the other side. The inhibitory potencies of the benzamide compounds were found to be sensitive to the nature and position of substituents on the benzamide ring, and can be rationalized on the basis of the structure of the HIV PR/**7** complex. These results partly confirm our initial hypothesis and suggest that optimal inhibitor designs should satisfy a requirement for providing polar interactions with Asp29 NH, and should minimize the conformational entropy loss on binding by reducing the number of freely rotatable bonds in inhibitors. Copyright © 1996 Elsevier Science Ltd

Introduction

Human immunodeficiency virus type 1 (HIV-1), a human retrovirus that causes AIDS,[1] encodes a protease that processes polyprotein precursors into viral structural proteins and replicative enzymes.[2] This processing is essential for the assembly and maturation of fully infectious virions.[3] Thus, the design of inhibitors of HIV-1 protease (HIV PR) is an important therapeutic goal in the treatment of AIDS. Numerous classes of potent peptidic inhibitors of HIV PR have been designed using the natural cleavage sites of the precursor polyproteins as starting points. These inhibitors are typically peptide substrate analogues in which the scissile P1–P1′ amide bond is replaced by a non-hydrolyzable isostere with tetrahedral geometry.[4] Peptidomimetics often make poor drugs owing to their potential adverse pharmacological properties; i.e., poor oral absorption, poor stability, and rapid metabolism.[5] C2 symmetry-based inhibitors have recently been designed to mimic the twofold symmetry of the active site of the enzyme as determined by X-ray crystal structure analysis of inhibitor/enzyme complex.[6] A-77003, XM-323, and ABT-538 represents several C2 symmetry-based inhibitors that have entered clinical trials in humans.[7] Recent studies have revealed the emergence of mutant strains of HIV that exhibit resistance toward these and other protease inhibitors.[8] The most deleterious mutation for A77003 is Arg to Gln at position 8(R8Q),[9] which affects the S3/S3′ subsite of the protease binding domain and increases the K_i of A-77003 by a factor of 165-fold.[10] We recently reported that the redesign of P3/P3′ residues of A-77003 can produce inhibitors which are equipotent towards both wild type enzyme and R8Q mutant protease.[11] Studies from several laboratories[12] show that inhibitors spanning only the S2–S2′ subsites can possess potent inhibitory activity. Thus, a sensible strategy for avoiding R8Q resistance is to truncate inhibitors while maintaining the crucial interactions necessary for strong binding. This approach has several potential benefits, since it would eliminate two or more peptide bonds, reduce molecular weight, diminish the potential for recognition by degradative enzymes, and result in improved activity against certain drug resistant strains. We recently reported the activity and utility of 2-methylbenzamides as conformationally-constrained P2/P2′ ligands for HIV PR inhibitors.[13] In this paper, we present a full account of our structure-guided effort to design novel and achiral phenylacetamides and benzamides as P2/P2′ groups in symmetry-based diol compounds along with the crystallographic structure of the HIV PR/**7** complex. We compare the inhibitory

†Present address: Departmento de Fisica, Universidad Nacional del Sur, 8000 Bahia Blanca, Argnetina.

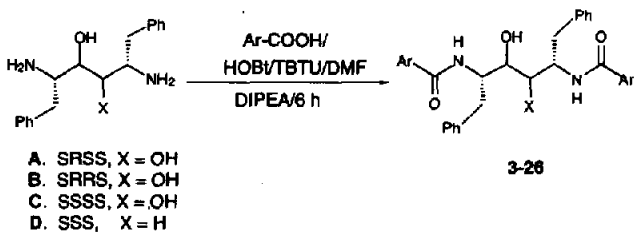

A. SRSS, X = OH
B. SRRS, X = OH
C. SSSS, X = OH
D. SSS, X = H

Scheme 1.

activity of these compounds against wild type and selected drug resistant mutant enzymes.

Chemistry

The inhibitor core unit for these studies, 2,5-diamino-1,6-diphenyl-3,4-hexanediol, was synthesized by McMurry coupling of natural Boc-phenylalaninal, and the diastereomers *SRSS*-**A**, *SRRS*-**B**, and *SSSS*-**C** were separated following a reported procedure.[14] The 2,5-diaminodiol **A** (X=*S*—OH) was condensed with suitably substituted benzoic acid using the TBTU/HOBt/DIPEA method to provide compounds **6–8**, and **15–24** (Scheme 1). Compounds **9–13** were prepared similarly by the condensation of the suitably substituted benzoic acids with the *SRRS*-diol **B** and compound **14** was prepared from benzoic acid and the *RSSR*-diol **C**. Condensation of 2,5-diaminodiol **A** (X=*S*—OH) with suitably substituted phenylacetic acid using the above procedure provided phenylacetamides **3–5**. The ethers **20a** and **21a** were prepared by the reaction of methyl 3-hydroxybenzoate with corresponding halides in the presence of NaH, followed by saponification (Scheme 2). The 3-hydroxy-5-methylbenzoic acid (**17a**) was prepared from sodium acetopyruate following a reported procedure.[15] The deshydroxy compounds **25** and **26** were prepared by condensation of *SSS*-2,5-diamino-1,6-diphenyl-3-hexanol[16] (**D**, X=H) with a suitably substitute benzoic acid using the TBTU/HOBt/DIPEA method (Scheme 1).

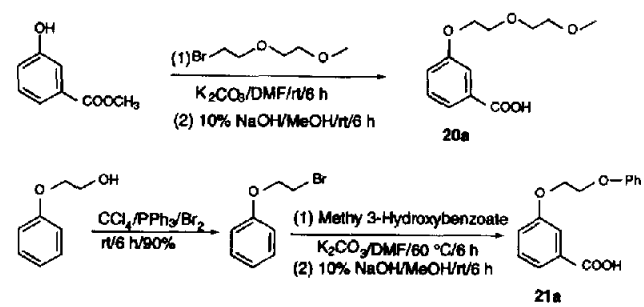

Scheme 2.

Design and Modeling

Crystallographic studies on the structure of the HIV PR/**1** complex revealed that the P2/P2′ carbamate oxygen atoms of **1** are involved in water-mediated

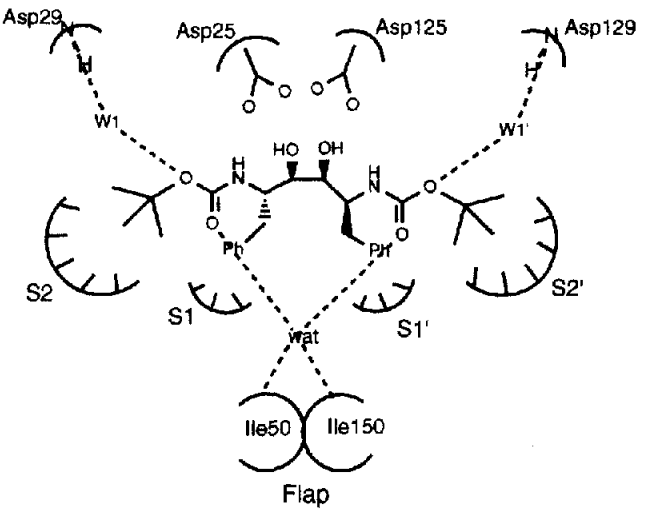

Figure 1. Cartoon representation of the interactions of compound **1** (red) with HIV PR active site. The hydrogen bonds are drawn in blue dashed lines. W1 and W′ are waters.

hydrogen bond with the Asp29 NH atom of the enzyme (Fig. 1).[17] In longer inhibitors spanning the P3–P3′ subsites of the enzyme the positions of these waters are usually occupied by carbonyl oxygen atoms from the backbone amide groups which form direct hydrogen bonding interactions with the Asp29/129 NH atoms.[6a,b] Polar interactions with Asp29/129 NH have also been shown to be crucial for the binding of several short inhibitors such as KNI272,[12a] and L-700,417[12b,c] to HIV PR. Modeling studies using the crystal structure of the HIV PR/**1** complex indicated that substitution the P2/P2′ group by the aromatic ring of a phenylacetamide group could offer a novel approach for accessing S2/S2′ subsites. The unsubstituted phenylacetamide derivative **3** was about 1000-fold less potent than **1** owing to the inability of **3** to satisfy the hydrogen bonding requirement in the S2/S2′ subsites. Visual examination of compound **3** in the HIV PR active site suggested that interactions with Asp29/129 NH could be achieved by addition of a polar group in the *ortho*-position of the aromatic ring of the phenylacetamide group. However, introduction of a hydroxyl group into either the *ortho* (**5**) or *meta* (**6**) positions resulted in only a marginal improvement in protease inhibition (Table 1). This lack of activity enhancement was attributed to the entropic cost of the two freely rotatable bonds of the phenylacetamide beyond the carbonyl. The elimination of these rotatable bonds was achieved through the design of benzamide analogues.

Modeling studies of the unsubstituted benzamide **6** in the HIV PR active site indicated that a hydrogen bond acceptor group in the *meta*-position of the benzamide ring should be optimal for hydrogen bonding to Asp29/129 NH. A model of complex consisting of the hydroxy-containing inhibitor **7**, a tetrahedrally coordinated water molecule that stabilizes the interaction of the inhibitor with the flap, and all enzyme residues within 6 Å of the inhibitor were energy minimized using the program SYBYL.[18] The aromatic 3-OH benzamide ring of **7** occupies the S2/S2′ subsites of the

enzyme and the *meta*-hydroxy groups were predicted to be within hydrogen bonding distance to the Asp29/129 NH (Fig. 2). Somewhat surprisingly, the benzamide rings had moved out of the amide plane by ca. 15°, probably to maximize both the interactions of the amide carbonyls with the flap water, and of the 3-OH groups with the Asp29/129 NH atoms. Conformational analysis performed in vacuo using *N*-methyl 3-hydroxybenzamide indicated a weak rotational barrier of 0.56 kcal/mol for the observed conformation of **7**, with the preferred conformation being one in which the orientation of the amide carbonyl and benzene ring are co-planar. We believed that this rotational barrier could be readily overcome and synthesized compounds **6** and **7** to test this hypothesis. Indeed, compounds **6** and **7** were both potent inhibitors of HIV PR with K_i values of 42 and 22 nM, respectively (Table 2). The 3-amino-benzamide derivative **19** exhibited a K_i value of 5 nM. In contrast, the *para*-hydroxy derivative **8** had a K_i value of 276 nM, while the 2-hydroxybenzamide analogue **9** was inactive. Subsequent studies indicated that stabilization of the nonplanar conformation by adding a 2-methyl substituent further enhanced the potency of the benzamides.[13]

Table 1. Influence of substituents linked to the central core on the in vitro activity[a]

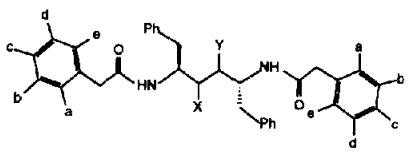

Compd	a	b	c	d	e	X	Y	% Inhib[b]	K_i (nM)
1	*N*-*tert*-butyloxycarbonyl					R-OH	S-OH		12
2	*N*-benzyloxycarbonyl					R-OH	S-OH		26
3	H	H	H	H	H	R-OH	S-OH	38	
4	H	OH	H	H	H	R-OH	S-OH		3000
5	OH	H	H	H	H	R-OH	S-OH	66	

[a]Inhibition of HIV PR was measured using a fluorogenic substrate.[21]
[b]Percent inhibition at 10 μM.

The influence of the stereochemistry of the diol core on the inhibitory potencies of a longer P3–P3′ series is documented;[6] in that series, the compounds possessing the *RS*- and *SS*-diol cores were more active, than compounds possessing the *RR*-diol core. A similar trend was observed in the present series (compare **7**, **14**, and **11**). For the *RR*-diol containing inhibitors **10–13** (Table 2) the presence of a polar group in the benzamide ring was essential for inhibition of HIV PR, compare the *RR*-**10**, which was inactive, with **11** which possesses a 3-hydroxybenzamide and exhibited a K_i value of 79 nM. Irrespective of the stereochemistry of the core diols (*RR* or *RS*) the 2-hydroxybenzamide-containing inhibitors **9** and **13** were inactive, whereas the 4-hydroxybenzamide-containing inhibitors **8** and **12** exhibited moderate inhibitory activities, $K_i = 276$ and 330 nM, respectively. The 3 log difference in the potency of **6** and **10** was unexpected and may be due to the participation of the aromatic ring in polar interactions.[19] The exact influence that the stereochemistry of the diol core (*RR* versus *RS*) has on the P2/P2′ benzamide conformation awaits crystallographic analysis.

Large variations in activity were also observed for different aromatic ring substituents or substitution patterns. The substitution of the 3-hydroxy group with

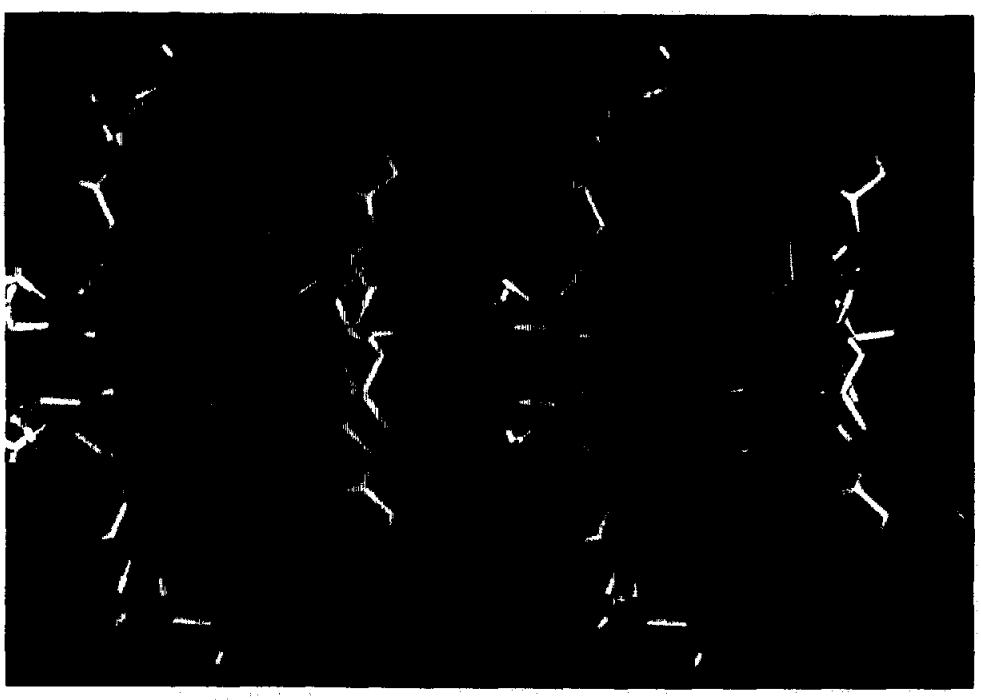

Figure 2. Steroview of a model of the inhibitor **7** (pink) in the HIV PR active site (colored by type). Proposed hydrogen bonds between the inhibitor **7** and the enzyme active site are shown in blue lines.

a nitro group (**24**), provided a poor inhibitor of HIV PR. The addition of hydrophilic groups in the 3,4-positions of the aromatic ring of the benzamide group led to a fourfold decrease in potency (compare **6** versus **15**), whereas the addition of hydroxy groups in the 3,5-positions caused a dramatic loss in inhibitory potency (compare **6** versus **16**). Etherification of the 3-OH group (compounds **20** and **21**) did not improve potency. Fusion of the second ring (compounds **22** and **23**) reduces inhibitor potency. Unlike the 2-methyl substitutions,[13] methylation at the 4- and 5-positions (compounds **17** and **18**, respectively) were not well tolerated in the 3-hydroxybenzamides.

Table 2. Influence of substituents linked to the central core on the in vitro activity[a]

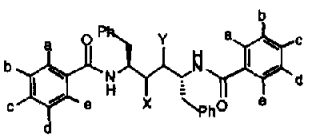

Compd	a	b	c	d	e	X	Y	% Inhib[b]	K_i (nM)
6	H	H	H	H	H	R-OH	S-OH		42
7	H	OH	H	H	H	R-OH	S-OH		22
8	H	H	OH	H	H	R-OH	S-OH		276
9	OH	H	H	H	H	R-OH	S-OH	32	
10	H	H	H	H	H	R-OH	R-OH	55	
11	H	OH	H	H	H	R-OH	R-OH		79
12	H	H	OH	H	H	R-OH	R-OH		330
13	OH	H	H	H	H	R-OH	R-OH	66	
14	H	OH	H	H	H	S-OH	S-OH		43

[a]Inhibition of HIV PR was measured using a fluorogenic substrate.[21]
[b]Percent inhibition at 10 μM.

HIV PR/7 complex

X-ray crystallographic analysis of the refined 2.1 Å resolution structure of the HIV PR complexed with the 3-hydroxybenzamide **7** revealed that the inhibitor binds in an extended conformation, as expected, spanning from the S2 to S2′ subsites of the enzyme. Two quasi-twofold symmetric orientations of the inhibitor were observed; these are related by a rotation around the twofold axis of the enzyme. The *R*-hydroxyl group of the inhibitor core is located close to the twofold axis, making a symmetric interaction with the active site aspartates 25/125, while the *S*-hydroxyl group makes only one hydrogen bond with the carboxylate group of the active site aspartates. A water molecule, usually observed in the peptidic inhibitors coordinated to the carbonyl oxygens of the inhibitor and amide nitrogens of the flap Ile50/150 residues,[19b] is also observed in this complex. The electron density for the 3-hydroxybenzamide group indicates that the 3-hydroxyphenyl groups are interacting asymmetrically with the S2/S2′ subsites of the enzyme (Fig. 3). On one side the 3-OH group of the benzamide ring (A ring) makes hydrogen bonding interactions with Asp29 NH (2.82 Å) as predicted from modeling studies, whereas on the other side (B ring) it interacts with Gly148 CO (2.98 Å, Fig. 4). The substituted aromatic ring of the P2/P2′ benzamides and the amide group are not co-planar in the crystal structure with **7**. The aromatic benzamide ring is 10° out of plane on the side that interacts with Asp29 NH, and is 46° out of plane on the side that interacts with Gly148.

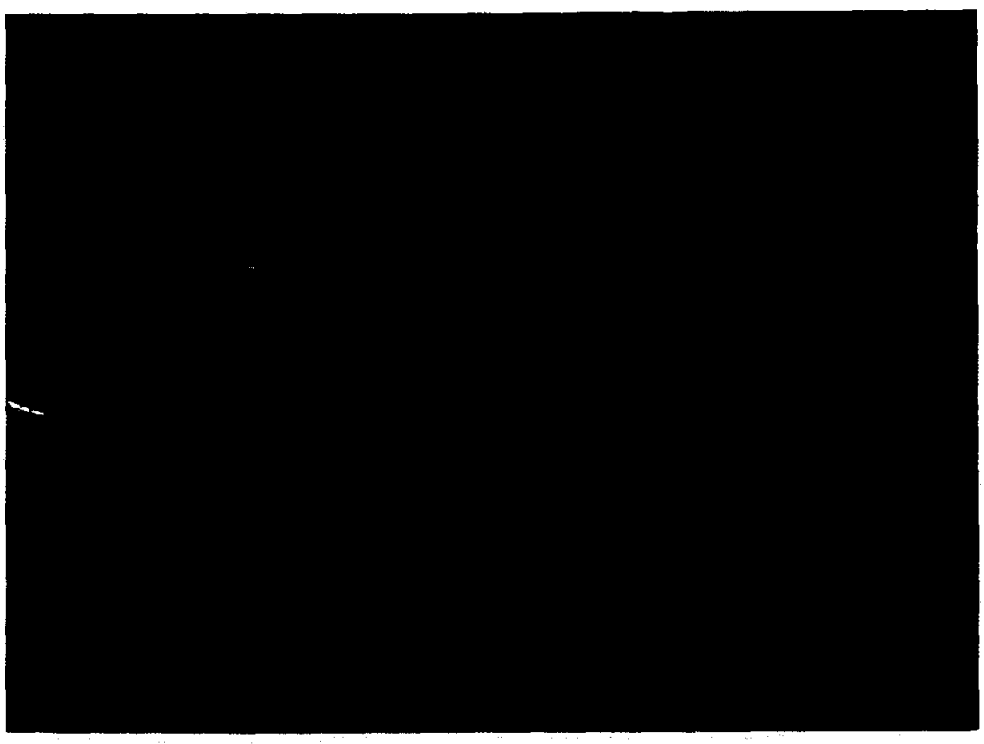

Figure 3. Stereoview of the $2F_o$-F_c map contoured at a 0.75 σ level (blue). F_o-F_c map contoured at a 2.0 σ level (red), with the phases calculated excluding the inhibitor. Atoms of the HIV PR active site and the inhibitor are colored by type.

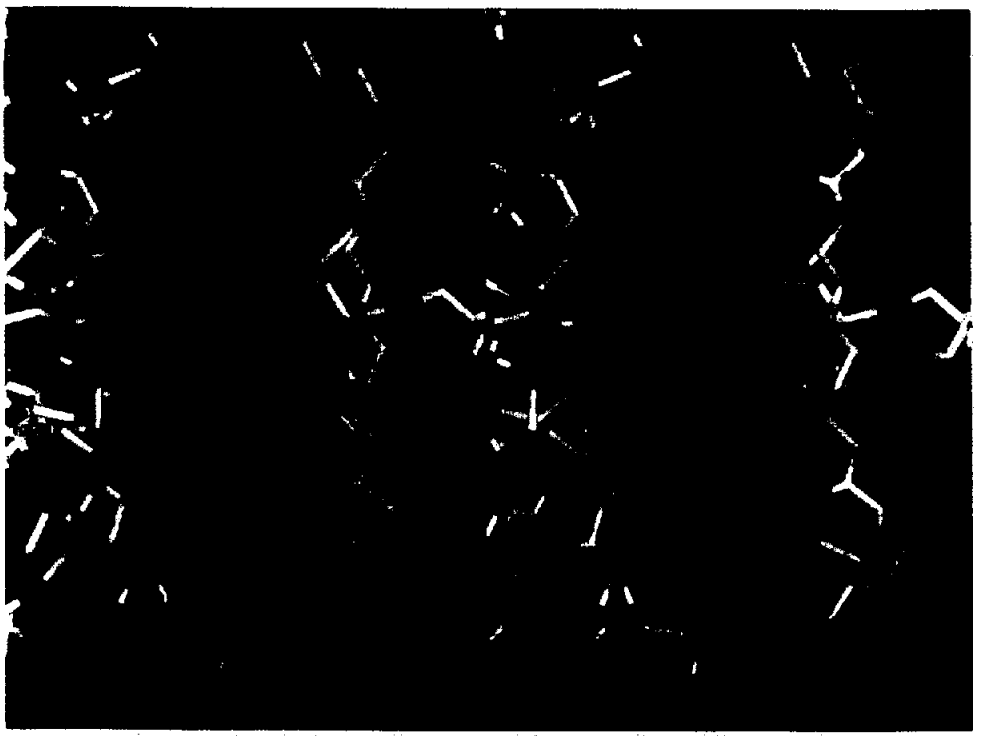

Figure 4. Stereoview of the HIV PR/**7** complex showing the two quasi-twofold asymmetric orientation of the inhibitor **7**. Atoms of the inhibitor **7** are colored pink and orange and the atoms of HIV PR are colored by type. Important hydrogen bonding interactions are shown in blue lines. HIV PR chain A residues are numbered 1–99 and the chain B residues are numbered 101–199.

The aromatic B-ring makes van der Waals contacts with Ile50, Ile147, Val132, and Ala128, and the aromatic A-ring interacts with Ile150, Ile47, and Ala28. A comparison of the HIV PR/**1**[17] and HIV PR/**7** structures reveal that the A-ring 3-OH group of **7** is within 1 Å of the bridging water molecule in the former, confirming the design strategy. The interactions of the central P1–P1′ diol core with the enzyme are similar to those observed with other compounds possessing this core.[20]

Many of the SAR trends can be readily rationalized based on the HIV PR/**7** structure (Fig. 4). The dramatic loss in the enzyme inhibitory potencies of the 2-OH derivatives **9** and **13** may be due to the inability of the hydroxyl group to form favorable hydrogen bonds with the Asp29 NH and/or Gly48 carbonyl in the S2/S2′ subsite of the HIV PR. Moderate PR inhibition by the 4-hydroxybenzamide analogues **8** and **12** may arise from their ability to interact with the Asp30/130 side chain carboxylate groups. The inactivity of the 3-nitrobenzamide analogue **24** may be due to the excessive volume of the nitro group. In the case of the bis-*meta*-substituted benzamides **16** and **17**, one of the substituents on the benzamide ring might project too deep into the mostly hydrophobic S2/S2′ pocket, thus causing unfavorable interactions. The decreased inhibitory potencies of ethers **20** and **21** may be due to a combination of factors such as their inability to act as hydrogen bond donors as well as to steric hindrance. Finally, deletion of the core *S*-hydroxy group of the diol core has been shown to improve the binding affinities compared with their diol counterparts.[16b] Surprisingly, the incorporation of a deshydroxy core did not improve the inhibitory potencies for this series of inhibitors (Table 3, **7** versus **25** and **19** versus **26**).

The inhibitory potencies of four selected compounds against R8Q and V82I HIV PR mutants are reported in Table 4. The activity against the wild type is also incorporated for comparison. The R8Q mutation mainly affects the P3/P3′ subsite on the enzyme. As these inhibitors do not contain P3/P3′ ligands, they were all equipotent against the R8Q mutant. The V82I mutation mostly affects S1/S1′ subsites of the enzyme. Inhibitor **19** exhibited about a 21-fold decrease in the inhibitory potency against the V82I mutant, whereas the potency of compound **7** was only slightly affected.

Conclusions

We have described a structure-based approach for the design of a template to produce specific interactions with the backbone NH of Asp29. The design led to the identification of the achiral, nonpeptidic 3-OH/NH_2-benzamide group as a novel P2/P2′ ligand. Crystallographic studies on the HIV PR/**7** complex suggest that the 3-OH/NH_2-benzamide ring system simultaneously provides good hydrophobic interactions and is involved in as many as two hydrogen bonds. The inhibitors were designed to be equipotent against wild type and R8Q mutant enzymes. The SAR data suggests that, in addition to the interactions with active site aspartates Asp25/125 and Ile50/150, additional polar interactions with the S2/S2′ subsite residues of the enzyme are

Table 3. Influence of substituents linked to the central core on the in vitro activity[a]

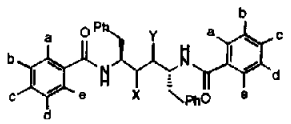

Compd	a	b	c	d	e	X	Y	% Inhib[b]	K_i (nM)
6	H	H	H	H	H	R-OH	S-OH	42	
7	H	OH	H	H	H	R-OH	S-OH		22
15	H	OH	OH	H	H	R-OH	S-OH		80
16	H	OH	H	OH	H	R-OH	S-OH		700
17	H	OH	H	CH_3	H	R-OH	S-OH		1000
18	H	OH	CH_3	H	H	R-OH	S-OH		132
19	H	NH_2	H	H	H	R-OH	S-OH		5
20	H	OR*[c]	H	H	H	R-OH	S-OH	63	
21	H	OR**[d]	H	H	H	R-OH	S-OH	9	
22		*N*-2-(4-oxo-4*H*-1-benzopyran)carbonyl				R-OH	S-OH	67	
23		*N*-2-(4-Hydroxyquinoline)carbonyl				R-OH	S-OH	31	
24	H	NO_2	H	H	H	R-OH	S-OH	40	
25	H	OH	H	H	H	S-OH	H		25
26	H	NH_2	H	H	H	S-OH	H		6

[a]Inhibition of HIV PR was measured using a fluorogenic substrate.[21]
[b]Percent inhibition at 10 μM.
[c]R* = $CH_2CH_2OCH_2CH_2OCH_3$.
[d]R** = CH_2CH_2OPh.

essential to achieve potent inhibition of HIV PR for this series of compounds.

Experimental

Chemistry

All melting points were recorded on a Electrothermal Digital Melting Point Apparatus (Model IA9200) and are uncorrected. Proton nuclear magnetic resonance (^{1}H NMR) spectra were recorded on a Varian XL-200 or VXR-500S MHz spectrometer. ^{1}H NMR spectral data are reported in δ ppm scale relative to TMS. High-resolution MS were recorded on a VG70–250 and FABMS on a VG ZAB-2F (Manchester, England) mass spectrometer. Flash chromatography was performed on silica gel (230–400 mesh, E. Merck). HPLC analysis were carried out using a Hewlett Packard 1050 chromatograph using a methanol:water (0.05% TFA) mixtures as mobile phase (gradient 50–100% of methanol over 30 min) on either (V): Vydac-Pack ODS-218 TP(C18) (250 × 4.6 mm, S-5 μm) reverse-phase column or (Y): YMC-Pack ODS-AQ (C18) (250 × 4.6 mm, S-5 μm, 120 Å) reverse-phase column. TLC was performed on silica gel F-254 plates (0.25; Whatman) and visualized using sulfuric acid or chlorine or ninhydrin/TDM (4,4′-tetramethyldiaminodiphenylethane) and UV methods. The following TLC solvent systems are used: (a) ethyl acetate:hexane (1:1), (b) chloroform:methanol (95:5), (c) chloroform:methanol (91:1), (d) chloroform:methanol:diisopropylamine (90:10:5), (e) acetone, (f) ethyl acetate:methanol:acetic acid (95:3:2), (g) ethyl acetate:hexane (7:3), and (h) chloroform:methanol (3:1). All solvents used were of reagent grade.

Table 4. Comparison of in vitro activity of select compounds with R8Q and V82I mutants[a]

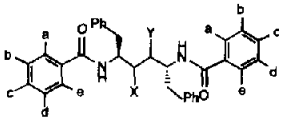

Compd	a	b	c	d	e	X	Y	WT	R8Q[b]	V82I[b]
7	H	OH	H	H	H	R-OH	S-OH	22	36	51
15	H	OH	OH	H	H	R-OH	S-OH	80	40	235
19	H	NH_2	H	H	H	R-OH	S-OH	5	20	109
26	H	OH	H	H	H	S-OH		25	34	96

[a]Inhibition of wild (W) and mutant HIV PR was measured using a fluorogenic substrate.[21]
[b]Inhibitions are in nM.

3-[2-[(Methoxy)ethoxy]ethoxy]benzoic acid (20a, Scheme 2). A mixture of 240 mg (1.6 mmol) of methyl 3-hydroxybenzoate, 200 mg of anhyd K_2CO_3 and 0.27 mL (2 mmol) of 1-bromo-2-(2-methoxyethoxy)ethane in DMF was heated with stirring at 50 °C for 6 h. After which the DMF was evaporated under reduced pressure, and the residue was extracted with ethyl ether. Methanol (5 mL) and NaOH (2 mL) was added to the above methyl benzoate and stirred at room temperature for 4 h. The methanol was removed under reduced pressure, and the residue washed with ethyl ether (5 mL), acidified, and extracted with ethyl acetate (3 × 10 mL). The combined ethyl acetate layer was washed with brine, dried, and evaporated to provide **20a** (300 mg, 79%) as a thick liquid; ^{1}H NMR ($CDCl_3$): δ 3.4 (s, 3H), 3.5 (m, 2H), 3.7 (m, 2H), 3.9 (m, 2H), 4.2 (m, 2H), 7.16 (m, 1H), 7.36 (m, 1H), 7.62 (m, 1H) and 7.69 (m, 1H).

3-[2-(Phenoxy)ethoxy]benzoic acid (21a, Scheme 2). To a stirred and cooled solution of triphenyl phosphene (1.9 g, 7.2 mmol), in anhyd methylene chloride (5 mL), under argon, a solution of bromine (0.7 mL) in CCl_4 (2 mL) was added slowly over 15 min. The stirring was continued for 30 min, after which, 2-phenoxyethanol (1 g, 7.2 mmol) in CH_2Cl_2 (2 mL) was added slowly. Reaction mixture was allowed to warm to room temperature and left overnight. The excess of solvents were stripped off and the residue was repeatedly extracted with petroleum ether. Evaporation of petroleum ether gave 2-phenoxyethyl bromide (1.4 g, 75%); ^{1}H NMR ($CDCl_3$): δ 3.66 (m, 2H), 4.30 (m, 2H) and 6.9–7.4 (m, 5H).

2-Phenoxyethyl bromide was converted to 3-[2-(phenoxy)ethoxy]benzoic acid (**21a**) by following an analogous procedure as described for **20a**; MS: *m/z* 258 $(M+Na)^+$; ^{1}H NMR ($CDCl_3$): δ 4.3 (m, 4H), 6.9–7.0 (m, 6H), 7.2–7.5 (m, 3H) and 12.5 (s, 1H).

Representative procedure for the preparation of bisamides

(2*S*,3*R*,4*S*,5*S*)-2,5-Bis[*N*-[(3-hydroxyphenyl)carbonyl]-amino]-3,4-dihydroxy-1,6-diphenyl hexane (7, Scheme 1). A solution of 102 mg (0.73 mmol) of 3-hydroxybenzoic acid, 214 mg (0.67 mmol) of 1*H*-benzatriole-1-yl-1,1,3,3-tetramethyluronium tetrafluoroborate (TBTU), 112 mg (0.73 mmol) of 1-hydroxybenzotriazole (HOBt), 172 mg (1.34 mmol, 233 μL) of diisopropylethyl amine (DIPEA), and 100 mg (0.33 mmol) of 2*S*,3*R*,4*S*,5*S*-2,5-diamino-3,4-dihydroxy-1,6-diphenyl hexane (**A**) in 10 mL of dimethylformamide (DMF) was stirred at room temperature for 1.5 h. After which the reaction was quenched with a drop of 4-(2-aminoethyl)morpholine. The solvent and volatiles were removed under reduced pressure, the residue taken up in ethyl-acetate and washed sequentially with 10% $KHSO_4$, water, aq $NaHCO_3$, brine dried, and concentrated in vacuo. The crystallization of crude product from methanol:water (1:10) gave 140 mg (78%) of **7** as a white solid: mp 102–104 °C; TLC [R_f=0.24 (B); 0.25 (G)]; HPLC [column V, t_R (retention time)=11.2 min]; MS: *m/z* 541 $(M+H)^+$; ^{1}H NMR (CD_3OD): δ 2.9 (d, J=7.6 Hz, 4H), 3.3 (m, 2H), 3.5 (s, 2H), 4.66 (t, J=7.4 Hz, 2H), 6.88–7.27 (m, 18Hz).

The compounds **3–26** were prepared following the analogous procedure.

(2*S*,3*R*,4*S*,5*S*)-2,5-Bis[*N*-(phenylacetyl)amino]-3,4-dihydroxy-1,6-diphenyl hexane (3). Mp 202–203 °C; TLC [R_f=0.38 (C); 0.67 (G)]; HPLC (column Y, t_R=21.1 min); MS: *m/z* 537 $(M+H)^+$; ^{1}H NMR (CD_3OD): δ 2.7 (m, 1 H), 2.86 (m, 1H), 2.89 (m, 1H), 2.94 (m, 1H), 3.32 (m, 4H), 3.37 (m, 1H), 3.43 (s, 2H), 3.6 (m, 1H), 4.0 (m, 2H), 6.9–7.25 (m, 20H).

(2*S*,3*R*,4*S*,5*S*)-2,5-Bis[*N*-[(3-hydroxyphenyl)acetyl]-amino]-3,4-dihydroxy-1,6-diphenyl hexane (4). Mp 203–205 °C; TLC [R_f=0.39 (B); 0.80 (G)]; HPLC (column V, t_R=11.4 min); MS: *m/z* 569 $(M+H)^+$; ^{1}H NMR (CD_3OD) δ 2.6 (m, 1H), 2.9 (m, 3H), 3.26 (d, J=3.5 Hz, 2H), 3.3 (m, 4H), 3.3–3.5 (m, 4H), 3.55 (dd, J=9.5, 1.0 Hz, 1H), 4.4 (m, 1H), 4.5 (m, 1H), 4.9 (m, 1H), 6.4 (m, 1H), 6.55 (m, 2H), 6.6 (m, 3H), 6.9–7.0 (m, 2H), 7.2 (m, 10H).

(2*S*,3*R*,4*S*,5*S*)-2,5-Bis[*N*-[(2-hydroxyphenyl)acetyl]-amino]-3,4-dihydroxy-1,6-diphenyl hexane (5). Mp 86–87 °C; TLC [R_f=0.20 (A); 0.41 (B)]; HPLC (column V, t_R=14.4 min); MS: *m/z* 591 $(M+Na)^+$; ^{1}H NMR (CD_3OD): δ 2.6 (m, 1H), 2.85 (m, 3H), 3.2 (m, 2H), 3.4 (m, 4H), 4.4–4.6 (m, 2H), 4.7 (m, 2H), 6.65–6.85 (m, 6H), 6.9 (m, 2H), 7.0–7.2 (m, 10H).

(2*S*,3*R*,4*S*,5*S*)-2,5-Bis[*N*-(phenylcarbonyl)amino]-3,4-dihydroxy-1,6-diphenyl hexane (6). Mp 224–225 °C; TLC [R_f=0.27 (A); 0.69 (C)]; HPLC (column Y, t_R=19.9 min); MS: *m/z* 509 $(M+H)^+$; ^{1}H NMR (DMSO-d_6): δ 2.79–2.95 (m, 1H), 2.97–3.10 (m, 3H), 3.45–3.50 (m, 1H), 3.61–3.67 (m, 1H), 4.49–4.65 (m, 2H), 5.14 (d, J=4.5 Hz, 1H), 5.33 (d, J=7.8 Hz, 1H), 7.06–7.53 (m, 6H), 7.68–7.71 (m, 2H), 7.77–7.78 (m, 2H), 8.00 (d, J=9.0 Hz, 1H), 8.12 (d, J=9.4 Hz, 1H).

(2*S*,3*R*,4*S*,5*S*)-2,5-Bis[*N*-[(4-hydroxyphenyl)carbonyl]-amino]-3,4-dihydroxy-1,6-diphenyl hexane (8). Mp 148 °C (dec); TLC [R_f=0.46 (C); 0.33 (E)]; HPLC (column Y, t_R=10.9 min); MS: *m/z* 541 $(M+H)^+$; ^{1}H NMR (CD_3OD): δ 2.77–2.85 (m, 1H), 2.98–3.08 (m, 3H), 3.65–3.75 (m, 2H), 4.67–4.88 (m, 4H), 6.76–6.88 (m, 4H), 7.05–7.36 (m, 12H), 7.61–7.64 (m, 1H), 7.76–7.79 (m, 1H).

(2*S*,3*R*,4*S*,5*S*)-2,5-Bis[*N*-[(2-hydroxyphenyl)carbonyl]-amino]-3,4-dihydroxy-1,6-diphenyl hexane (9). Mp 87–88 °C; TLC [R_f=0.57 (G); 0.82 (H)]; HPLC (column Y, t_R=20.3 min); MS: *m/z* 541 $(M+H)^+$; ^{1}H NMR (DMSO-d_6): δ 2.81–2.87 (m, 2H), 2.91–2.95 (m, 1H), 3.02–3.06 (m, 1H), 3.36–3.40 (m, 1H), 3.58–3.61 (m, 1H), 4.43–4.48 (m, 1H), 4.55–4.60 (m, 1H), 5.19 (m, 1H), 5.25–5.26 (m, 1H), 6.69 (dt, J=8.8, 2.0 Hz, 2H), 6.75 (dt, J=8.8, 2.0 Hz, 2H), 7.06–7.09 (m, 1H), 7.13–7.19 (m, 3H), 7.23–7.27 (m, 4H), 7.31–7.33 (m, 2H), 7.56–7.59 (m, 2H), 7.66–7.68 (m, 2H), 7.73 (d, J=9.0 Hz, 1H), 7.89 (d, J=8.9 Hz, 1H), 9.83(s, 1H), 9.96 (s, 1H).

(2*S*,3*R*,4*R*,5*S*)-2,5-Bis[*N*-(phenylcarbonyl)amino]-3,4-dihydroxy-1,6-diphenyl hexane (10). Mp 178–179 °C; TLC [R_f=0.40 (A); 0.64 (B)]; HPLC (column V, t_R=14.1 min); MS: *m/z* 509 $(M+H)^+$; ^{1}H NMR (DMSO-d_6): δ 2.9 (m, 4H), 3.3 (d, J=4.8 Hz, 2H), 3.4 (s, 2H), 4.7 (m, 2H), 7.1 (m, 2H), 7.2 (m, 4H), 7.4 (m, 4H), 7.7 (m, 4H), 7.9 (m, 2H).

(2*S*,3*R*,4*R*,5*S*)-2,5-Bis[*N*-[(3-hydroxyphenyl)carbonyl]-amino]-3,4-dihydroxy-1,6-diphenyl hexane (11). Mp 113–115 °C; TLC [R_f=0.40 (B); 0.28 (D)]; HPLC (column V, t_R=9.2 min); MS: *m/z* 541 $(M+H)^+$; ^{1}H NMR (CD_3OD): δ 2.8–2.9 (m, 2H), 3.3 (m, 2H), 3.6 (s, 1H), 3.7 (s, 1H), 4.3–4.4 (m, 2H), 6.88–7.27 (m, 18H).

(2*S*,3*R*,4*R*,5*S*)-2,5-Bis[*N*-[(4-hydroxyphenyl)carbonyl]-amino]-3,4-dihydroxy-1,6-diphenyl hexane (12). Mp 120–121 °C; TLC [R_f=0.28 (A); 0.54 (B)]; HPLC (column V, t_R=9.2 min); MS: *m/z* 541 $(M+H)^+$; ^{1}H NMR (acetone-d_6): δ 2.1 (s, 2H), 3.0 (m, 4H), 3.5 (s, 2H), 4.0 (m, 2H), 4.7 (m, 2H), 6.8–7.3 (m, 14H), 7.7 (m, 4H).

(2*S*,3*R*,4*R*,5*S*)-2,5-Bis[*N*-[(2-hydroxyphenyl)carbonyl]-amino]-3,4-dihydroxy-1,6-diphenyl hexane (13). Mp 79–80 °C; TLC [R_f=0.28 (D); 0.64 (F)]; HPLC (column V, t_R=16.1 min); MS: *m/z* 541 $(M+H)^+$; ^{1}H NMR (acetone-d_6): δ 2.9 (m, 4H), 3.0 (m, 2H), 3.6 (s, 2H), 4.45 (s, 2H), 4.95 (m, 2H), 6.89 (m, 4H), 7.04 (m, 2H), 7.1 (m, 4H), 7.3 (m, 4H), 7.7 (m, 4H).

(2*S*,3*S*,4*S*,5*S*)-2,5-Bis[*N*-[(3-hydroxyphenyl)carbonyl]-amino]-3,4-dihydroxy-1,6-diphenyl hexane (14). Mp 155–160 °C; TLC [R_f=0.10 (A); 0.44 (C)]; HPLC (column V, t_R=13.7 min); MS: *m/z* 541 $(M+H)^+$; ^{1}H NMR (CD_3OD): δ 2.22 (s, 3H), 2.26 (s, 3H), 2.80–2.95 (m, 1H), 2.96–3.09 (m, 3H), 3.3 (m, 2H), 3.34 (s, 1H), 3.7 (m, 2 H), 4.65 (m, 2H), 6.6–6.8 (m, 4H), 6.9 (m, 2H), 7.1–7.3 (m, 10H).

(2*S*,3*R*,4*S*,5*S*)-2,5-Bis[*N*-[(3,4-dihydroxyphenyl)carbonyl] amino]-3,4-dihydroxy-1,6-diphenyl hexane (15). Mp 134–135 °C; TLC [R_f=0.11 (B); 0.66 (F)]; HPLC (column V, t_R=7.4 min); MS: *m/z* 573 $(M+H)^+$; ^{1}H NMR (CD_3OD): δ 2.7–2.9 (m, 2H), 3.0 (m, 2H), 3.3 (m, 4H), 3.65 (dd, *J*=8.5, 3.0 Hz, 1H), 3.5–3.7 (m, 2H), 6.7–6.8 (m, 2 H), 6.9–7.4 (m, 14H).

(2*S*,3*R*,4*S*,5*S*)-2,5-Bis[*N*-[(3,5-dihydroxyphenyl)carbonyl] amino]-3,4-dihydroxy-1,6-diphenyl hexane (16). Mp 136–137 °C; TLC [R_f=0.10 (B); 0.62 (F)]; HPLC (column V, t_R=7.5 min); MS: *m/z* 573 $(M+H)^+$; ^{1}H NMR (CD_3OD): δ 2.9 (d, *J*=7.6 Hz, 4H), 3.3 (m, 2H), 3.5 (s, 2H), 4.66 (t, *J*=7.4 Hz, 2H), 6.88–7.27 (m, 18H).

(2*S*, 3*R*, 4*S*, 5*S*)-2, 5-Bis[*N*-[(3-hydroxy-5-methylphenyl)-carbonyl]amino]-3,4-dihydroxy-1,6-diphenyl hexane (17). Mp 129–131 °C; TLC [R_f=0.45 (B); 0.40 (F)]; HPLC (column Y, t_R=16.8 min); MS *m/z*: 569 $(M+H)^+$; ^{1}H NMR (CD_3OD): δ 2.22 (s, 3H), 2.26 (s, 3H), 2.8–2.95 (m, 1H), 2.96–3.09 (m, 3H), 3.3 (m, 2H), 3.34 (s, 1H), 3.7 (m, 2H), 4.65 (m, 2H), 6.6–6.8 (m, 4H), 6.9 (m, 2H), 7.1–7.3 (m, 10H).

(2*S*, 3*R*, 4*S*, 5*S*)-2, 5-Bis[*N*-[(3-hydroxy-4-methylphenyl) carbonyl]amino]-3,4-dihydroxy-1,6-diphenyl hexane (18). Mp 126–127 °C; TLC [R_f=0.54 (G); 0.60 (H)]; HPLC (column V, t_R=19.7 min); MS: *m/z* 569 $(M+H)^+$; ^{1}H NMR (CD_3OD): δ 2.1 (d, *J*=6 Hz, 6H), 2.85 (m, 2H), 3.0 (m, 2H), 3.3 (m, 2H), 3.6 (m, 2H), 4.6 (m, 4H), 6.96–7.35 (m, 16H).

(2*S*,3*R*,4*S*,5*S*)-2,5-Bis[*N*-[(3-aminophenyl)carbonyl]-amino]-3,4-dihydroxy-1,6-diphenyl hexane (19). The mixture of **25** (60 mg, 0.1 mmol) and 10 mg of 10% palladium on carbon in 15 mL of ethanol was stirred vigorously under H_2 atmosphere for 24 h. The resulting mixture was filtered and concentrated in vacuo to provide 52 mg (94%) of **20**: mp 94–95 °C; TLC [R_f=0.32 (D); 0.42 (E)]; HPLC (column V, t_R=5.4 min); MS: *m/z* 539 $(M+H)^+$; ^{1}H NMR (CD_3OD): δ 2.8 (m, 1H), 3.0–3.12 (m, 3H), 3.4 (a, *J*=7.0 Hz, 1H), 3.65 (dd, *J*=8.5, 3.0 Hz, 1H), 3.73 (dd, *J*=8.5, 1.0 Hz, 1H), 4.65 (m, 1H), 6.9 (m, 2H), 7.0–7.2 (m, 16 H).

(2*S*,3*R*,4*S*,5*S*)-2,5-Bis[*N*-[[3-[2-[(methoxy)ethoxy]ethoxy]phenyl]carbonyl]amino]-3,4-dihydroxy-1,6-diphenyl hexane (20). Mp 171–172 °C; TLC [R_f=0.13 (G); 0.75 (H)]; HPLC (column Y, t_R=19.8 min); MS: *m/z* 767 $(M+H)^+$; ^{1}H NMR (CD_3OD): δ 2.9 (m, 1H), 3.1 (m, 3H), 3.5–3.6 (m, 4H), 3.6–3.7(m, 6H), 3.7–3.8 (m, 4H), 4.0–4.1 (m, 4H), 4.6 (m, 2H), 6.9–7.4 (m, 18H).

(2*S*,3*R*,4*S*,5*S*)-2,5-Bis[*N*-[[3-[2-(phenoxy)ethoxy]phenyl] carbonyl]amino]-3,4-dihydroxy-1,6-diphenyl hexane (21). Mp 151–152 °C; TLC [R_f=0.31 (A); 0.76 (C)]; HPLC (column Y, t_R=21.7 min); MS: *m/z* 781 $(M+H)^+$; ^{1}H NMR ($CDCl_3$): δ 2.9 (m, 1H), 3.3 (m, 3H), 3.6 (m, 4H), 4.05 (m, 1H), 4.1 (m, 3H), 4.8 (m, 2H), 5.0 (m, 2H), 6.65–6.8 (m, 2H), 6.85 (m, 6H), 6.95 (m, 3H), 7.0–7.15 (m, 6H), 7.15–7.3 (m, 7H), 7.3 (m, 1H), 7.8 (m, 1H).

(2*S*,3*R*,4*S*,5*S*)-2,5-Bis[*N*-[2-(4-oxo-4*H*-1-benzopyran)-carbonyl]amino]-3,4-dihydroxy-1,6-diphenyl hexane (22). Mp 230–231 °C; TLC [R_f=0.61 (C); 0.80 (F)]; HPLC (column Y, t_R=20.2 min); MS: *m/z* 645 $(M+H)^+$; ^{1}H NMR (DMSO-d_6): δ 2.8–3.1 (m, 4H), 3.7 (m, 2H), 4.6 (m, 2H), 5.2 (m, 1H), 5.7 (m, 1H), 6.6 (s, 1H), 6.7 (s, 1H), 7.1–7.3 (m, 10H), 7.5 (m, 2H), 7.8–7.9 (m, 4H), 8.0 (m, 2H), 8.0 (m, 2H).

(2*S*, 3*R*, 4*S*, 5*S*)-2, 5-Bis[*N*- [2- (4-hydroxyquinoline) carbonyl]-amino]-3,4-dihydroxy-1,6-diphenyl hexane (23). Mp 179–180 °C; TLC [R_f=0.52 (C); 0.30 (F)]; HPLC (column Y, t_R=18.5 min); MS: *m/z* 643 $(M+H)^+$; ^{1}H NMR (DMSO-d_6): δ 2.85 (m, 1H), 3.0 (m, 3H), 3.66 (m, 2H), 4.6 (m, 2H), 5.05–5.87 (m, 2H), 7.1–7.35 (m, 12H), 7.5–8.2 (m, 8H), 8.6 (m, 2H), 11.6 (m, 2H).

(2*S*,3*R*,4*S*,5*S*)-2,5-Bis[*N*-[(3-nitrophenyl)carbonyl]-amino]-3,4-dihydroxy-1,6-diphenyl hexane (24). Mp 220–221 °C; TLC [R_f=0.20 (A); 0.66 (C)]; HPLC (column Y, t_R=21.3 min); MS: *m/z* 599 $(M+H)^+$; ^{1}H NMR (CD_3OD): δ 2.9 (m, 1H), 3.1 (m, 3H), 3.6 (m, 1H), 4.1 (m, 1H), 7.0–8.6 (m, 18H).

(2*S*,3*S*,5*S*)-2,5-Bis[*N*-[(3-hydroxyphenyl)carbonyl]-amino]-1,6-diphenyl-3-hydroxy hexane (25). Mp 99–101 °C; TLC [R_f=0.34 (D); 0.43 (E)]; HPLC (column Y, t_R =14.9 min); MS: *m/z* 525 $(M+H)^+$; ^{1}H NMR (CD_3OD): δ 1.7 (m, 2H), 2.9 (m, 4H), 3.3 (m, 1H), 3.8 (m, 1H), 4.4 (m, 2H), 6.9 (m, 2H), 7.0–7.3 (m, 16 H).

(2*S*,3*S*,5*S*)-2,5-Bis[*N*-[(3-aminophenyl)carbonyl]-amino]-1,6-diphenyl-3-hydroxy hexane (26). Mp 113–114 °C; TLC [R_f=0.35 (D); 0.51 (E)]; HPLC

(column Y, t_R=9.5 min); MS: *m/z* 545 $(M+Na)^+$; ^1H NMR (CD_3OD): δ 1.8 (m, 2H), 2.9 (m, 4H), 3.3 (m, 2H), 3.8 (m, 1H), 4.3 (m, 2H), 7.0–7.3 (m, 18H).

HIV protease inhibition assay

The IC_{50} and K_i values for the compounds were determined using purified wild type and mutant HIV PR in a fluorogenic assay as previously described.[21]

Crystallization

For co-crystallization, the HIV PR at a concentration of 6 mg/mL, in 50 mM sodium acetate, pH 5.6, and 10 mM dithiotreitol, was mixed with **7** in a 1:5 molar ratio to a final dimethyl sulfoxide concentration of 5%. Crystals were grown at room temperature by the hanging drop method. The well mix consisted of 0.3 M ammonium sulphate, pH 6.0, 0.5% β-octylglucoside, 5% methanol, and 5% *n*-octanol. Macroseeding in sitting drops was performed to grow larger crystals, adding 5% ethanol to the original well mix for the seeding step. The procedure was repeated with the new macroseeds to produce crystals of data collection quality.

X-ray data collection and structure refinement

X-ray diffraction data were collected from a single rod-shaped crystal, using an R-Axis II image plate detector (Rigaku Co., Japan). The X-ray source was a RU200 (Rigaku Co., Japan) rotating anode generator operated at 5.0 kW, with a 0.3 × 0.3 mm nominal focus size, a 0.3 mm collimator and a graphite monochromator. The crystal-to-detector distance was set to 100 mm. Data extending to 2.1 Å resolution were collected, on a total of 60 frames, with an oscillation angle of 1.0° and an exposure time of 60 min per frame. The space group of the crystal is P61, with cell constants $a=b=63.48$, $c=83.65$ Å and one dimer per asymmetric unit. $R_{merge}=8.43\%$ for 10,455 independent reflections out of 25,032 total accepted observations. The data set was 93.1% complete at 2.5 Å resolution and 90.8% complete at 2.08 Å resolution. A total of 9038 reflections in the 10.0 to 2.1 Å resolution range with $F/\sigma(F) > 1.0$ was used for refinement. The refined model includes the protein, two pseudo-twofold symmetric orientations of the inhibitor and 98 water molecules. The *R* value for the refined model is 18.4%, and the RMSD between model and idealized geometry is 0.013 Å for bond length, 3.11° for bond angles and 28.8° for dihedral angles. The programs XPLOR[22] and QUANTA[23] were used for electron density map calculations, model refinement and visualization.

Acknowledgment

We thank Dr E. T. Baldwin for assistance with data collection.

References and Notes

1. Gallo, R. C.; Montagnier, L. *Sci. Am.* **1988**, *259*, 40.

2. (a) Jacks, T.; Power, M. D., Masiarz, R. R.; Luciw, P. A.; Barr, P. J.; Varmus, H. E. *Nature (London)* **1988**, *331*, 280; (b). Kay, J.; Dunn, B. *Biochem. Biophys. Acta* **1990**, *1048*, 1 .

3. (a) Kohl, N. E.; Emini, E. A.; Schleif, W. A.; Davis, L. J.; Heimbach, J. C.; Dixon, R. A. F.; Scolnick, E. M.; Sigal, I. S. *Proc. Natl. Acad. Sci. U.S.A* **1988**, *85*, 4686; (b) Peng, C.; Ho, B.; Chang, T.; Chang, N. *J. Virol.* **1989**, *63*, 2555; (c) Gottlinger, H.; Sodroski; J.; Haseltine, W. *Proc. Natl. Acad. Sci. U.S.A* **1989**, *86*, 5781.

4. (a) Moore, M. L.; Dreyer, G. B. *Perspect. Drug Dis. Design* **1993**, *1*, 85; (b). Tomasselli, A. G.; Howe, J.; Wlodawer, A.; Heinrikson, R. L. *Int. J. Chem Biotechnol.* **1991**, 6; (c). Huff, J. R. *J. Med. Chem.* **1991**, *34*, 2305; (d). Norbeck, D. W.; Kempf, D. J. *Ann. Rep. Med. Chem.* **1991**, *26*, 141; (e). Meek, T. D. *J. Enzyme Inhib.* **1992**, *6*, 65.

5. Plattner, J. J.; Norbeck, D. W. In *Drug Discovery Technologies*; Clark, C. R.; Moos, W. H., Eds.; Ellis Horwood: Chichester, 1990; pp 92–126.

6. (a) Erickson, J. W. *Perspect. Drug Dis. Design* **1993**, *1*, 109; (b) Erickson, J. W.; Neidhart, D. J.; VanDrie, J.; Kempf, D.; Wang, X. C.; Norbeck, D. W.; Plattner, J. J.; Rittenhouse, J. W.; Turon, M.; Wideburg, N.; Kohlbrenner, W. E.; Simmer, R.; Helfrich, R.; Paul, D. A.; Knigge, M. *Science* **1990**, *249*, 527; (c). Kempf, D. S.; Codacovi, L.; Wang, X. C.; Norbeck, D. W.; Kohlbrenner, N. E.; Wideburg, N.; Paul, D. A.; Knigge, M. F.; Vasavanonda, S.; Craig-Kennard, A.; Saldivar, A.; Rosenbrook, Jr W.; Clement, J. J.; Plattner, J. J.; Erickson, J. W. *J. Med. Chem.* **1990**, *33*, 2687; (d). Kempf, D. S.; Marsh, K.; Paul, D. A.; Knigge, M. F.; Norbeck, D.; Kohlbrenner, W. E.; Codacovi, L.; Vasavanonda, S.; Byrant, P., Wang, X. C.; Wideburg, N. E.; Clement, J. J.; Plattner, J. J.; Erickson, J. W. *Antimicrob. Agents Chemother.* **1991**, *35*, 2209.

7. Goldthorpe, S.; Kinchington, D.; Lovelidge, L. *Int. Antiviral News* **1995**, *3*, 92.

8. Erickson, J. W. *Nature Struct. Biol.* **1995**, *2*, 523.

9. Ho. D. D.; Toyoshima, T.; Mo, H.; Kempf, D. J.; Norbeck, D.; Chen, C.; Wideburg, N. E.; Burt, S. K.; Erickson, J. W.; Singh, M. K. *J. Virol.* **1994**, *68*, 2016.

10. Gulnik, S. V.; Suvorov, L. I.; Liu, B.; Yu, B.; Anderson, B.; Mitsuya, H.; Erickson, J. W. *Biochemistry* **1995**, *34*, 9282.

11. Majer, P.; Burt, S. K.; Gulnik, S.; Ho, D. D.; Erickson, J. W. *13th American Peptide Symposium.* Edmonton, Canada, 1993.

12. (a). Baldwin, E. T.; Bhat, T. N.; Gulnik, S.; Liu, B.; Topol, I. A.; Kiso, Y.; Mimoto, T.; Mitsuya, H.; Erickson, J. W. *Structure* **1995**, *3*, 581; (b) Lyle, T. A.; Wiscount, C. M.; Guare, J. P.; Thompson, W. J.; Anderson, P. S.; Darke, P. L.; Zugay, J. A.; Emini, E. A.; Schleif, W. A.; Quintero, J. C.; Dixon, R. A. F.; Sigal, I. S.; Huff, J. R. *J. Med. Chem.* **1991**, *34*, 1230; (c) Bone, R.; Vacca, J. P.; Anderson, P. S.; Holloway, M. K. *J. Am. Chem. Soc.* **1991**, *113*, 9382; (d). Kim, E. E.; Baker, C. T.; Dwyer, M. D.; Murcko, M. A.; Rao, B. G.; Tung, R. D.; Navia, M. A. *J. Am. Chem. Soc.* **1995**, *117*, 1181.

13. Randad, R. S.; Lubkowska, L.; Bhat, T. N.; Munshi, S.; Gulnik, S. V.; Yu, B.; Erickson, J. W. *Bioorg. Med. Chem. Lett.* **1995**, *5*, 1707.

14. Kempf, D. J.; Sowin, T. J.; Doherty, E. M.; Hannick, S. M.; Codacovi, L.; Henry, R. F.; Green, B. E.; Spanton, S. G.; Norbeck, D. W. *J. Org. Chem.* **1992**, *57*, 5692.

15. Turner, F. A.; Gearien, J. E. *J. Org. Chem.* **1959**, *24*, 1952.

16. (a) Stuk, T. L.; Haight, A. R.; Scarpetti, D.; Allen, M. S.; Menzia, J. A.; Robbins, T. A.; Parekh, S. I.; Langridge, D. C.; Tien, J. J.; Pariza, R. J.; Kerdesky, F. A. *J. Org. Chem.* **1994**, *59*, 4040; (b) Kempf, D. S.; Norbeck, D. W.; Codacovi, L.; Wang, X. C.; Kohlbrenner, N. E.; Wideburg, N.; Saldivar, A.; Craig-Kennard, A.; Vasavanonda, S.; Clement, J. J.; Erickson, J. W. In *Recent Advances in the Chemistry of Anti-infective Agents*; Bently, P. H.; Ponsford, R., Eds.; 1993; Royal Society of Chemistry: Cambridge; pp 297–313.

17. Hosur, M. V.; Bhat, T. N.; Erickson, J. W. Unpublished results. Preliminary accounts of this work: Randad, R. S.; Lubkowska, L.; Silva, A. M.; Bhat, T. N.; Gulnik, S. V.; Yu, B.; Erickson, J. W. *Abstracts of Papers*, 209th American Chemical Society: Anaheim, California, 1995; MED 112; Randad, R. S.; Lubkowska, L.; Silva, A. M.; Guerin, D. M. A.; Baldwin, E. T.; Gulnik, S. V.; Yu, B.; Erickson, J. W. *Abstracts of Papers*, Structural Biology of AIDS Related Systems: Bethesda, Maryland 1994.

18. The structure of **1** was modified to create **7**. Energy minimization was carried out using the Maxmin program and the Gasteiger-Marsili charges within the SYBYL. Minimization was carried out until the rms deviation for all atoms was less than 0.5 kcal/mol Å.

19. (a) Suzuki, S.; Green, P. G.; Bumgarner, R. E.; Dasgupta, S.; Goddard, III, W. A.; Blake, G. A. *Science* **1992**, *257*, 942; (b) Wlodawer, W.; Erickson, J. W. *Annu. Rev. Biochem.* **1993**, *62*, 543.

20. Hosur, M. V.; Bhat, N. T.; Kempf, D. J.; Baldwin, E. T.; Liu, B.; Gulnik, S.; Wideburg, N. E.; Norbeck, D. W.; Appelt, K.; Erickson, J. W. *J. Am. Chem. Soc.* **1994**, *116*, 847.

21. Kageyama, S.; Momoto, T.; Murakawa, Y.; Nomizu, M; Ford, H.; Shirasaka, T.; Gulnik, S.; Erickson, J. W.; Takada, K.; Hayashi, H.; Broder, S.; Kiso, Y. and Mitsuya, H. *Antimicrob. Agents Chemother.* **1993**, *37*, 272.

22. Brunger, A.T. *Ann. Rev. Phys. Chem.* **1991**, *42*, 197.

23. Molecular Simulations Inc. U.S.A.

(*Received in U.S.A.* 5 *October* 1995)